Uptake and Reaction Kinetics of Acetone, 2-Butanone, 2,4-Pentanedione, and Acetaldehyde in Sulfuric Acid Solutions

Williams Esteve and Barbara Nozière*

Rosenstiel School of Marine and Atmospheric Science, University of Miami, Miami, Florida 33149

Received: March 8, 2005; In Final Form: September 23, 2005

This work presents a study of the uptake of acetone, 2-butanone (methyl ethyl ketone), 2,4-pentanedione, and acetaldehyde by sulfuric acid solutions with an aim at understanding the reactivity of carbonyl compounds present in the atmosphere toward acidic aerosols. Experiments were performed in a rotating wetted-wall reactor coupled to a mass spectrometer at room temperature (298 ± 3 K) with 0−96 wt % H_2SO_4 solutions. For all compounds, a reactive uptake was observed at high acidity (≥64 wt % H_2SO_4). The corresponding reactions were found to follow a second-order kinetics, and their rate constants, k_{liq}^{II} (M^{-1} s^{-1}) were found to increase exponentially with acidity. These rate constants and their variations with acid concentration were in good agreement with the kinetic behavior of acid-catalyzed aldol condensation reported in the organic chemical literature, except for 2,4-pentanedione. The results of this work suggest that aldol condensation should be too slow to account for the enhanced organic aerosol mass observed in smog chamber studies and should have an even smaller contribution under atmospheric conditions. The rate constants of other compounds, such as large aldehydes, remain however to be measured. However, in order to contribute significantly to organic aerosol formation, a liquid phase reaction would have to result in an uptake coefficient of the order of 10^{-2}.

I. Introduction

For the past decade or so, numerous studies of the formation of secondary organic aerosols (SOA) suggested that these processes were best described by a reversible absorptive partitioning mechanism.[1] Recent validations of a regional model containing a state-of-the-art module for the simulation of these aerosols indicated, however, that this partitioning model almost systematically underestimates actual SOA masses.[2] Simultaneously, smog chamber studies have identified some processes that might explain the enhanced SOA mass in real aerosols: the uptake by and reaction of volatile organic compounds, such as carbonyls and alcohols, in acidic aerosols.[3−7] However, these studies did not allow the investigators to identify the specific reactions involved or to estimate their kinetics. A detailed understanding of the mechanism and kinetics is yet indispensable for an accurate description of these processes under atmospheric conditions. The organic chemical literature contains a large body of information on the mechanism and kinetics of the reactions of organic compounds in condensed media,[8,9] but little of it is relevant to atmospheric conditions. Some investigations of the uptake of acetone[10−14] and acetaldehyde[15] by sulfuric acid solutions from an atmospheric point of view have been performed. In the case of acetone, an irreversible reaction was observed in concentrated acid and unambiguously identified as aldol condensation thanks to specific products such as mesityl oxide and trimethyl benzene.[10,11] The purpose of the present work was to complete and generalize these studies by measuring the rates of these reactions for a range of acid compositions and various carbonyl compounds. In addition to allowing for the quantification of these reactions under a range of atmospheric conditions, the purpose of these data was to provide a general understanding of the reactivity of carbonyl compounds in acidic aerosols. The uptake of acetone, 2-butanone, 2,4-pentanedione, and acetaldehyde, expected to represent a wide range of reactivity, has thus been studied. The results were then compared with liquid phase studies reported in the organic chemical literature[16] to determine if the mechanism and kinetics established previously were also valid in atmospheric aerosols.

II. Experimental Section

The experimental setup used for this study is described here for the first time. It consists of a rotating wetted-wall (RWW) horizontal flow reactor coupled to an electron-impact ionization mass spectrometer (Figure 1). The principle of the rotated wetted-wall reactor has been established in previous works.[17,18] The main reactor is a Pyrex cylinder equipped with a jacket for thermostating and an inside rotating cylinder (20 mm i.d., 18 cm long). Small volumes of sulfuric acid solutions (typically 1.5 mL, corresponding to a liquid film depth of about 0.1 mm) were placed on the rotating walls. Rotating the inner cylinder at about 15 rpm ensured that the acid films were spread evenly on the walls. A glass rod placed along its bottom helped to spread the film on the walls. As it was rotating with the cylinder, this rod also provided a mixing of the solutions at a rate of about 0.25 s^{-1}. The carrier gas was mostly composed of N_2 and flowed through the reactor at a total flow between 100 and 400 sccm (corresponding to a flow velocity between 4 and 15 cm s^{-1} at 0.13 atm). A small flow of N_2 saturated in water vapor was added to this main flow so that the water content of the carrier gas was in equilibrium with the acid solutions.[19] For instance, the water vapor pressure was between 0 and 4×10^{-3} atm for acid compositions between 96 and 65 wt % H_2SO_4. This ensured that the acid composition was not modified during the experiments. This composition was checked before and after each experiment by standard titration methods using known solutions of NaOH and found to vary by less than 0.5 wt % H_2SO_4. A small flow of organic compounds diluted in N_2 was

* To whom correspondence should be addressed. E-mail: bnoziere@rsmas.miami.edu.

10.1021/jp051199a CCC: $30.25
Published on Web 11/10/2005

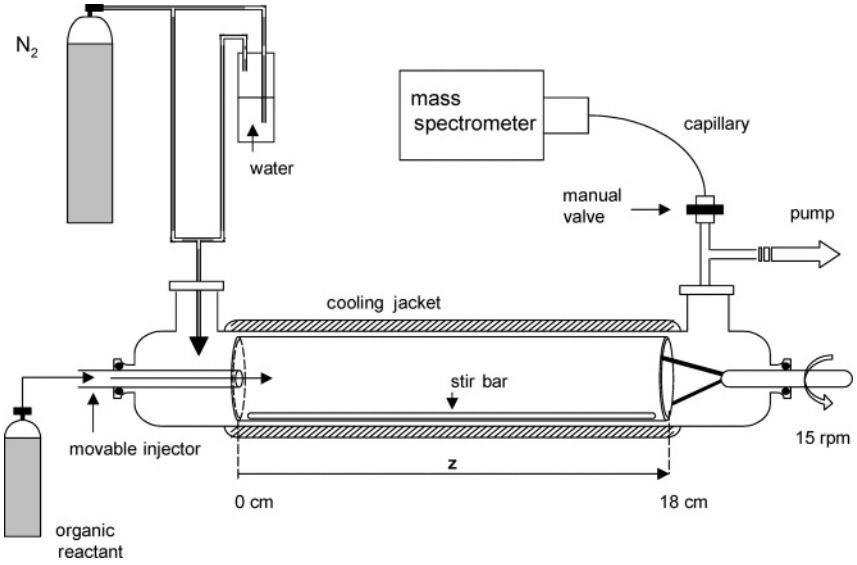

Figure 1. Schematics of the RWW reactor/mass spectrometer experimental setup.

introduced in the reactor through a movable injector. The partial pressures of organic compounds in the various experiments were between 10^{-5} and 10^{-4} atm. Most experiments were performed at a total pressure of 0.13 ± 0.011 atm, but a few were performed at 0.086 atm.

A small fraction of the outflow of the reactor ($\sim$1.5 sccm) was sampled into a commercial mass spectrometer (Hewlett-Packard 5971) via a fused silica capillary (50−100 cm long, 0.10 mm i.d., Supelco). Trace compounds present in this outflow were ionized by electron impact (energy = 70 eV) and detected after a quadrupole mass filter with an electron multiplier maintained at 2500 V. The two most abundant ions of each compound were monitored in single ion mode (SIM). For a carbonyl compound of molecular weight m, the major ions were typically the fragment corresponding to the release of a $-CH_3$ group, at $m - 15$ amu, and the molecular ion, m^+. Thus, acetone was monitored at 43 and 58 amu, 2-butanone at 57 and 72 amu, and 2,4-pentanedione at 85 and 100 amu. Acetaldehyde was monitored by its main ion at 44 amu, which overlapped with the main ion of CO_2. Traces of CO_2 in the system resulted in more uncertainties in the uptake measurements of acetaldehyde than for the other compounds. The linearity of the detection response of the system was investigated for partial pressures between 10^{-6} and 10^{-4} atm for each compound. For acetone, 2-butanone, and acetaldehyde, the response was linear. For 2,4-pentanedione, monitored at higher masses, the response was not linear and was best fitted by a second-order function, which was used to convert detection signals into concentrations when calculating the uptake.

Uptake experiments proceeded by first placing the injector beyond the acid film ($z \geq 18$ cm in Figure 1) to determine a baseline signal and then by pulling the injector back to expose the film to the organic compound ($0 \leq z \leq 18$ cm). The uptake coefficient, γ, measuring the fraction of molecules entering the solution, was calculated by comparing the organic concentrations obtained after exposure, C, to the baseline concentration, C_o:

$$\ln\left(\frac{C_o}{C}\right) = \frac{\gamma\omega}{2r}\tau \qquad (1)$$

where ω = molecular speed of the organic compound ($\sim 3 \times 10^4$ cm s^{-1}), r is the reactor radius (1 cm), and τ is the contact time (between 1 and 4 s), determined in the plug flow approximation. In the above equation, the ratio $2/r$ represents the specific surface of the liquid film in the reactor. Our experimental setup allowed measurements of uptake coefficients between 10^{-6} and 2×10^{-4}. At low acid concentrations, the uptake was time-dependent: The signal returned to the baseline after some time, indicating saturation of the solution by the organic compound (Figure 2a). Then, pushing the injector back to its initial position resulted in a second transient signal corresponding to the release of the organic molecules back to the gas phase and demonstrating that the uptake processes were reversible (Figure 2a). At high acidity, the uptake displayed a constant component (Figure 2b) and replacing the injector in its initial position did not lead to the release of molecules from the liquid. This type of uptake indicated the occurrence of thermodynamically irreversible reactions and is referred to as "reactive" uptake throughout this manuscript. In this case, placing the injector at different positions in the reactor showed that the signal was decreasing exponentially along the axis (Figure 3). This was expressed as an apparent first-order loss for the organic compound from the gas phase:

$$\ln\left(\frac{C_o}{C}\right) = k^I_{obs}\,\tau \qquad (2)$$

At intermediate acidity, where the uptake included both a reversible and a reactive component, the latter was measured as the constant offset between baseline and uptake signal obtained at long reaction time. The flow conditions were chosen so that reactive uptake was only limited by processes taking place in or at the surface of the solutions. In addition, experiments were performed below atmospheric pressure to limit the effects of gas phase diffusion on the uptake. A correction was applied to the data to take into account a potential contribution from gas phase diffusion:

$$\frac{1}{k^I_{gas}} = \frac{1}{k^I_{obs}} - \frac{1}{k_{diff}} \qquad (3)$$

where k_{diff} is the diffusion-limited rate:[20]

$$k_{diff} = \frac{3.6 \times D_{gas}}{r^2} \qquad (4)$$

and D_{gas} is the diffusion coefficient in the gas. Assuming that $D_{gas} = 0.1$ cm^2 s^{-1} for organic compounds at atmospheric

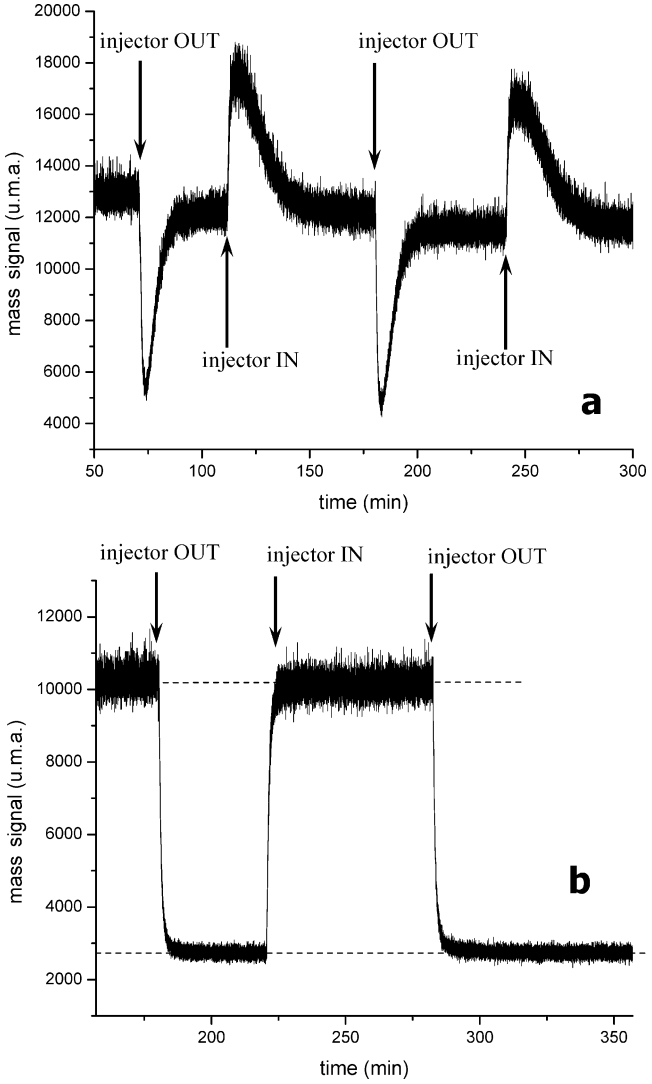

Figure 2. Typical experimental profiles for the (a) reversible uptake of acetone by 70 wt % H_2SO_4 solution and (b) irreversible uptake of acetone by 96 wt % H_2SO_4 solution.

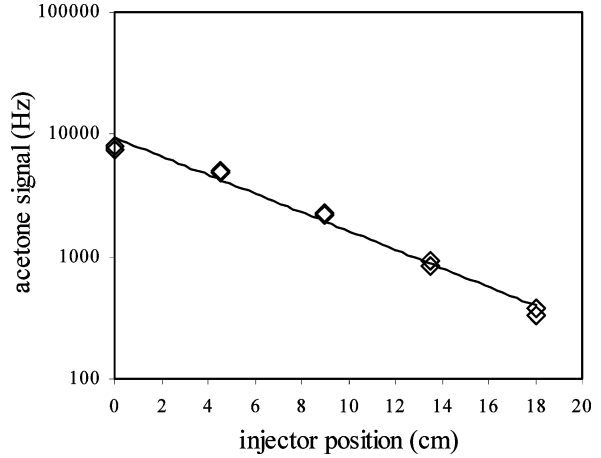

Figure 3. Acetone signal as a function of the position of the injector for 96 wt % H_2SO_4 solution at 298 K.

pressure[19] led to $D_{gas} \sim 0.76$ cm^2 s^{-1} and $k_{diff} \sim 2.74$ s^{-1} at 0.13 atm. As shown in Table 1, this correction had little effect on many of the data.

As will be seen below, the reactions were found to be slow in these experiments, and the liquid solutions were stirred. Both factors ensured that the concentration profiles of organic com-

TABLE 1: Uptake Coefficient, γ, Gas Phase Loss Rates Observed [k^I_{obs} (s^{-1})], and Corrected for Diffusion [k^I_{gas} (s^{-1})], Henry's Law Coefficients (H), Diffusion Coefficients (D_{liq}) Estimated from Ref 26, and First-Order Reaction Rates in Liquid [k^I_{liq} (s^{-1})] in Our Experiments[a]

	acetone						2-butanone						2,4-pentanedione						acetaldehyde					
wt % H_2SO_4	γ	k^I_{obs} (s^{-1})	k^I_{gas} (s^{-1})	H (Matm^{-1})	D_{liq} (cm^2 s^{-1})	k^I_{liq} (s^{-1})	γ	k^I_{obs} (s^{-1})	k^I_{gas} (s^{-1})	H	k^I_{liq} (s^{-1})	γ	k^I_{obs} (s^{-1})	k^I_{gas} (s^{-1})	H	k^I_{liq} (s^{-1})	γ	k^I_{obs} (s^{-1})	k^I_{gas} (s^{-1})	H	k^I_{liq} (s^{-1})
96					1.2×10^{-7}													9.4×10^{-6}	0.19	0.20	540	6.3×10^{-4}
90							7.7×10^{-5}	1.25	2.3	1220	*3.0 × 10^{-3}*											
89.4	5.2×10^{-5}	0.93	1.41	840	3.0×10^{-7}	*2.7 × 10^{-3}*																
85	5.6×10^{-6}	0.10	0.10	650	5.0×10^{-7}	2.5×10^{-4}						9.4×10^{-5}	1.28	2.41	3340	*1.9 × 10^{-3}*	4.2×10^{-7}	0.01	0.01	270	5.2×10^{-5}
80.8	4.7×10^{-6}	0.07	0.07	500	8.0×10^{-7}	2.3×10^{-4}	5.3×10^{-6}	0.09	0.09	720	2.0×10^{-4}	1.2×10^{-4}	1.53	3.47	2880	*1.9 × 10^{-3}*					
73.9	1.6×10^{-6}	0.03	0.03	320	1.0×10^{-6}	1.5×10^{-4}						9.2×10^{-5}	1.16	2.01	1830	*1.8 × 10^{-3}*					
70.3				290 (70%)*			1.1×10^{-6}	0.02	0.02	380	7.4×10^{-5}	1.2×10^{-5}	0.17	0.18	1400 (70%)*	2.0×10^{-4}				80 (68%)*	
63.9										230 (62%)*		2.3×10^{-6}	0.03	0.03	900	5.4×10^{-5}					
0				27*						22*					155*					16*	

[a] Each series of data is the average of 2−8 measurements. "*" are measured values. Italics: Values where the correction for gas phase diffusion is significant.

pounds in solutions were radially uniform and in equilibrium with the gas phase (see justifications in Appendix I). In this case, the rate for first-order losses of organic molecules in the liquid, k^{I}_{liq}, can be obtained from the gas phase rate loss, k^{I}_{gas}, by the following relationship:

$$k^{I}_{liq} = \frac{V_{gas}\, k^{I}_{gas}}{V_{liq} RTH} \tag{5}$$

where H is the Henry's law coefficient of the organic compound in solution, V_{gas} is the volume of gas ($\sim$59.7 cm^3), V_{liq} is the volume of solution, T is the temperature, and R is the gas constant (see demonstration of eq 5 in Appendix II). The advantage of this approach over nonstirred solutions or real particles is that, as shown in eq 5, the analysis does not require one to know the diffusion coefficients in the liquid (the coefficients given in Table 1 are for information only and are not used in the analysis). As detailed below, we had strong evidence in this study that the reaction kinetics was second order. The last step of the analysis was thus to determine second-order rate constants, k^{II}_{liq}, from the first-order rate constants, k_{liq}, given by eq 5. As demonstrated in Appendix III, this was achieved by dividing k_{liq} by the concentration of the organic compound at roughly mid-reactor:

$$k^{II}_{liq} = \frac{k^{I}_{liq}}{RTHC_o}\left[\frac{L\nu_{gas}}{1 - e^{-\nu_{gas}L}}\right] \tag{6}$$

where L is the length of the reactor and ν_{gas} is the slope of the first-order decay observed in Figure 3.

Bubble Column Experiments. Some of the main sources of uncertainties in the determination of reaction rate constants in this work are the Henry's law coefficients for organic compounds in sulfuric acid solutions. These coefficients have been measured previously at low temperatures for acetone[12−14] and acetaldehyde[15] and at room temperature for acetone and 2,4-pentanedione.[21] Because extrapolating coefficients from low temperatures to room temperature would have introduced large uncertainties in the present analysis, experiments have been performed to measure the Henry's law coefficients of 2-butanone and acetaldehyde at room temperature using the bubble column technique. This technique was described previously[21] and will only be briefly described here. It consists of placing a known volume V (20−25 mL) of solution of the organic compound in sulfuric acid (typical concentration $1-2 \times 10^{-2}$ M) in a glass column (170 mm high, 20 mm i.d.) through which nitrogen flowed. This flow induced a dilution of the organic concentrations in both gas and liquid phases, which was monitored by measuring the concentration of organic compounds in the gas in real time. For this, the bubble column was coupled to a gas chromatograph equipped with a FID detector (HP 5890) via a column (HP cross-linked methyl silicone gum, 12 m $\times$ 0.2 mm $\times$ 0.33 μm) maintained at 303 K. This dilution resulted in first order decays (of the order of 5×10^{-5} to 10^{-3} s^{-1}), the slope of which provided the value of the apparent Henry's law coefficient, H. These coefficients were measured for solution compositions between pure water and about 70 wt % H_2SO_4 for both compounds.

Chemicals and Standards Preparation. Standard mixtures of organic compound in N_2 (typically 2×10^{-4} atm) were individually prepared by injecting small quantities (200−350 μL) of the pure liquid compound into an evacuated cylinder and pressurizing with pure nitrogen to $P = 1000$ psig ($P \sim 68$ atm).[22] Sulfuric acid solutions were prepared by mixing 96 wt % H_2SO_4 with distillated water. The acid composition of these solutions was determined accurately by titration with known NaOH solutions. Sulfuric acid, Aldrich, 95−98 wt % H_2SO_4, ACS reagent; acetone, B & J, HPLC grade; 2-butanone, Aldrich, 99%; 2,4-pentanedione, Aldrich, 99+%; nitrogen, Airgas, ultrahigh purity.

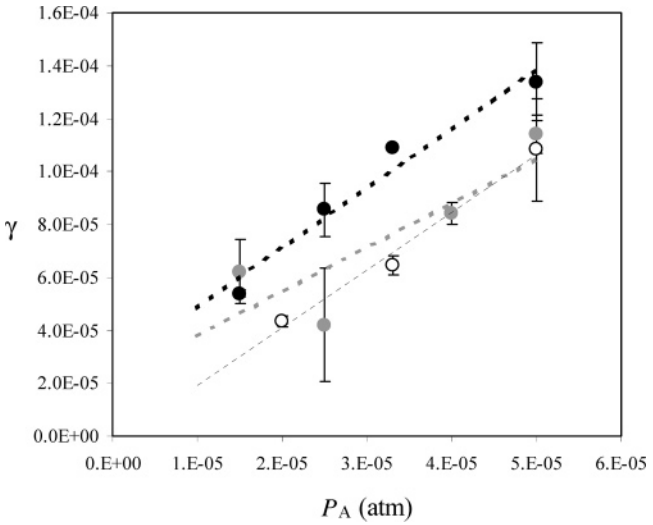

Figure 4. Variation of the uptake coefficient with partial pressure of organic (P_A) for acetone (full circles) and 2-butanone in 85 wt % H_2SO_4 (open circles) and for 2,4-pentanedione in 80 wt % H_2SO_4 (grey circles). Error bars represent the standard deviation on 2−4 measurements.

III. Results

The uptake of acetone, 2-butanone, 2,4-pentanedione, and acetaldehyde was investigated over the whole range of sulfuric acid composition, 0−96 wt % H_2SO_4 at room temperature (298 $\pm$ 2 K). For all compounds, the uptake was reversible at low and intermediate acid concentrations but displayed a reactive component beyond a certain concentration: 74 wt % for acetone, 70 wt % for 2-butanone, 64 wt % for 2,4-pentanedione, and 85 wt % for acetaldehyde.

In a first series of experiments, the reactive uptake of acetone, 2-butanone, and 2,4-pentanedione was measured as a function of the partial pressure of organic reactants between 1 and 5 $\times$ 10^{-5} atm, in 80−85 wt % solutions and at 298 $\pm$ 3 K. The results are shown in Figure 4. For all three compounds, a linear increase of the uptake with the partial pressure of reactant was evident and indicated that the reactions followed a second order (note that for acetaldehyde the large uncertainties on the uptake made this study inconclusive). However, the large uncertainties at low partial pressures (due to the small differences between baseline and uptake signals) did not allow us to conclude the presence of nonzero intercepts and, therefore, of first-order kinetic components as well. However, because two previous kinetic studies of the reactions of carbonyl compounds in acid already established that the kinetics was strictly second order,[11,16] we have used this assumption in the remainder of the analysis.

In a second series of experiments, the reactive uptake of each compound was measured at room temperature over the range of acid concentration where it could be observed. First-order loss rates in the gas, k^{I}_{obs}, were measured, and second-order rate constants, k^{II}_{liq} (M^{-1} s^{-1}), were determined according to the analysis explained previously. The results, as well as values for the important parameters of the analysis, are given in Table 1 (again, the diffusion coefficients are for information only and

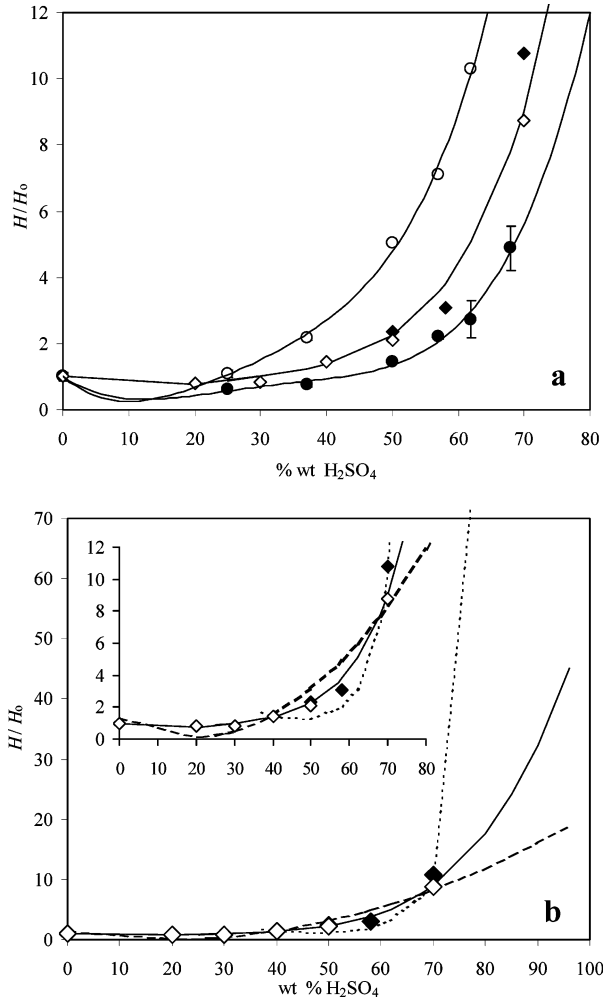

Figure 5. Relative Henry's law coefficients for 2-butanone (open circles) and acetaldehyde (full circles), as compared to the ones reported by ref 21 for acetone (open diamonds) and 2,4-pentanedione (full diamonds). The lines represent the fits to the data (see text).

TABLE 2: Henry's Law Coefficients for 2-Butanone and Acetaldehyde at 298 ± 3 K (in M atm^{-1}) as a Function of Sulfuric Acid Composition Measured by the Bubble Column Technique

wt % H_2SO_4	*H*(acetaldehyde)	*H*(2-butanone)
0	16.4 ± 1.9	22.4 ± 1.9
25	10.1 ± 0.2	24.4 ± 2.1
37	12.3 ± 0.8	48.4 ± 1.5
50	23.5 ± 0.5	112.5 ± 0.7
57	36.3 ± 1.1	159 ± 5
62	44.6 ± 9.3	230 ± 5
68	79.7 ± 11.1	

are not part of the analysis). Each series of data is the average of 2−8 measurements.

The Henry's law coefficients for acetaldehyde and 2-butanone in sulfuric acid 0−68 wt % measured by the bubble column technique are shown in Table 2 where the errors reflect statistical dispersion on the measurements only. These coefficients, normalized by their values in water, H/H_o, are compared with the relative coefficients reported previously for acetone and 2,4-pentanedione[21] in Figure 5a. All of these compounds become very reactive in concentrated solutions, and their Henry's law coefficients are difficult to measure beyond 70 wt % H_2SO_4. However, the analysis of the present work required values for these coefficients precisely in this upper acid range. Because the physicochemical processes responsible for the increase of

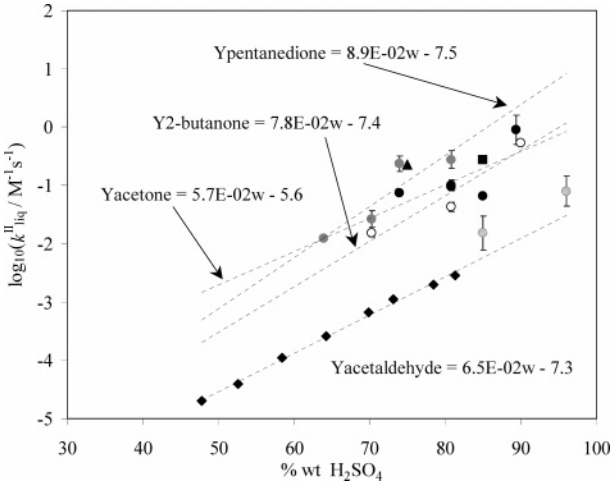

Figure 6. Second-order rate constants as a function of sulfuric acid concentration for acetone (full circles), 2-butanone (open circles), 2,4-pentanedione (dark gray circles), and acetaldehyde (pale gray circles). The lines are the linear regressions on the experimental values. Comparison with rate constant for aldol condensation of acetaldehyde from ref 16 (full diamonds) and for acetone at 200 (full triangle) and 220 K (full square) from ref 11.

these coefficients with acidity (protonation, aldolization...) are still open to debate,[12−15,21] there is currently no reliable theoretical model on which to base an extrapolation to concentrated solutions. In the absence of such theoretical basis, the empirical approach of using the curve fitting best the measured values over 0−70 wt % was chosen. Figure 5b compares various fitting curves and justifies the choice of a fourth-order function over other functions. The coefficients obtained by this extrapolation and used in our analyses are given in Table 1 so that, if better estimates become available, the rate constants determined in this work can be corrected accordingly. However, to reflect the large uncertainties made in these extrapolations, exponential uncertainties have been attributed to the results of the present work. These uncertainties have been calculated from the experimental error on the measured Henry's coefficient (∼20%) raised to the power of the ratio between the measured value and the extrapolated one. For example, the highest measured value of *H*(acetone) is 290 Matm^{-1} in 70 wt %. The error on the extrapolated value *H*(89.4 wt %) = 840 is $(\times 1.2)^{2.9}/(1.2)^{2.9}$ = ×1.7/1.7, and the corresponding error interval is (500−1430) Matm^{-1}. Similarly, the largest errors on the coefficients of each compound (in Matm^{-1}) were *H*(acetone, 96 wt %) = 1220 × 2.1/2.1, *H*(butanone, 96 wt %) = 1670 × 3.8/3.8, *H*(pentanedione, 85 wt %) = 3340 × 1.5/1.5, and *H*(acetaldehyde, 96 wt %) = 540 × 3.4/3.4.

The values of $k_{II_{liq}}$ obtained from these estimated Henry's law coefficients were between 10^{-2} and 1 M^{-1} s^{-1} and are presented as a function of acid composition in Figure 6. Despite the uncertainties, these results indicate an exponential increase of $k_{II_{liq}}$ with acidity. The slope (in logarithmic scale) is very similar for all of the compounds studied

$$\log_{10}(k^{II}_{liq}) = (6.6 \pm 2.0) \times 10^{-2} \times w + C \qquad (7)$$

Uncertainties on the slope include 30% of uncertainties from the linear regressions and 5% of dispersion between the slopes obtained with different compounds. The constants *C* obtained for each compound were between −7.5 and −5.6 and are reported in Table 3, where uncertainties include the 30% for the linear regression and the systematic errors on the Henry's law coefficients.

TABLE 3: Enolization Constants (K_{enol}) and Acidity Constants (K_{H+}) for the Carbonyl Compounds Studied in This Work[a]

	K_{enol}	K_{H+} (M)	$7.5 + \log(K_{enol}/K_{H+})$	C
acetaldehyde	5.2×10^{-7} (27)	4.7×10^{8} (16)	−7.5	-7.3 ± 4.0
acetone	6.0×10^{-7} (28)	2.3×10^{5} (31)	−4.1	-5.6 ± 3.8
2-butanone	3.1×10^{-8} (29)	2.6×10^{5} (30)	−6.7	-7.4 ± 3.3
2,4-pentanedione	4 (30)	2.5×10^{4} (32)	+3.7	-7.5 ± 3.4

[a] Comparison of the constant $7.5 + \log(K_{enol}/K_{H+})$ with the constant C obtained from uptake measurements.

IV. Discussion

Although aldol condensation is a widely known class of reaction in organic chemistry,[8,9] few studies have focused on the acid-catalyzed mechanism. The only one, to our knowledge, uses the reaction of acetaldehyde as an illustration.[16] Although the acid ranges studied do not overlap, there is a very good agreement between the results of both studies (Figure 6), the rate constants measured in this work overestimating the ones expected from ref 16 by about 30%, which is within the uncertainties. This agreement provides a validation of our measurements and of the analysis used in this work.

More importantly, the rate constants measured in this work allow for a comparison with the mechanism and kinetics previously established.[16] This mechanism involves four steps: (i) protonation

$$\underset{\text{“A”}}{R-C(O)-R'} + H^+ \leftrightarrow \underset{\text{“AH}^+\text{”}}{R-C^+(OH)-R'} \qquad K_{H+} = a_A a_{H+}/a_{AH+} \quad (8)$$

(ii) enolization

$$\underset{\text{“A”}}{R-C(O)-R'} \leftrightarrow \underset{\text{“enol”}}{R_{-H}=C(OH)-R'} \qquad K_{enol} = a_{enol}/a_A \quad (9)$$

(iii) addition

$$R-C^+(OH)-R' + R_{-H}=C(OH)-R' \leftrightarrow R-C(OH)(R')-R_{-H}-C(O)-R' + H^+ \qquad K_{add} \quad (10)$$

and (iv) dehydration

$$R-C(OH)(R')-R_{-H}-C(O)-R' \leftrightarrow R-C(O)(R_{-H}')-R_{-H}-C(O)-R' + H_2O \qquad K_{dehyd} \quad (11)$$

where the K_i represents the equilibrium constant of each step and a_i is the activity of species i in solution. All of these steps are thermodynamically reversible, but because of the small concentration of water in concentrated acid, step iv becomes completely displaced toward dehydration as the acid concentration increases. The irreversibility of step iv at high acidity is responsible for the irreversibility of the whole chemical system in concentrated solutions observed in this work and in previous ones.

Another important result of previous studies is that the kinetically limiting step of the mechanism is the addition, step iii, and is second order.[16] This second order has since then been confirmed for acetone[11] and in this work by the increase of the uptake coefficient with partial pressure of the reactant observed with acetone, 2-butanone, and 2,4-pentanedione.

The kinetic study of ref 16 proposes the following expression for the rate constant of the overall reaction at 298 K:

$$\log_{10}(k_{aldol}/k_o) = \log_{10}(K_{enol}/K_{H+}) + \log_{10}(C_{H+} \times a_{H_2O}) + mX \quad (12)$$

where C_{H+} is the concentration of proton, a_{H_2O} is the activity of water, m is a proportional factor ($m \sim 1$), and X is the excess acidity of the solution.[23] This expression can be compared to the results of the present work by converting C_{H+} and a_{H_2O} in wt % H_2SO_4 scale using the aerosol inorganic model[24] and replacing X by its equivalent in wt % H_2SO_4.[23] The value for the parameter k_o, the rate constant in pure water, is not known for other compounds than acetaldehyde. The same value has thus been used for all carbonyl compounds: $k_o = 1.2 \times 10^6$ M^{-2} s^{-1}.[16] Equation 12 then simplifies into:

$$\log_{10}(k_{aldol}) = 6.5 \times 10^{-2} \times w + 7.5 + \log_{10}(K_{enol}/K_{H+}) \quad (13)$$

where w = acid composition in wt % H_2SO_4. Equation 13 thus allows the calculation of the rate constant for aldol condensation of any carbonyl compound in any acid concentration, provided that the enolization and acidity constants of this compound, K_{enol} and K_{H+}, are known. The slope of this equation might, however, vary with the type of acid, as it reflects the catalytic efficiency of the solvent.

The comparison of k_{aldol} and eq 13 with k_{liq}^{II} and eq 7 shows obvious similarities (Figure 6). For all compounds, the agreements between the slopes of both equations are good, especially considering the uncertainties on the Henry's law coefficients in the present work. A comparison of the intercept values measured for eq 7 with the ones predicted for eq 13 is made in Table 3. The agreement is again very good for acetone, 2-butanone, and acetaldehyde, further validating the measurements made in this work and confirming that the reactions observed in this work were indeed aldol condensation. For 2,4-pentanedione, however, the measured intercept (and thus the rate constants) is much lower than the one predicted by eq 13. 2,4-Pentanedione has been studied in this work precisely because its K_{enol} is exceptionally high (see Table 3), which, according to eq 13, should result in a very fast reaction. A possible explanation for the discrepancy is that for compounds with such stable enols, the addition step (iii) might be fast or, at least, not kinetically limiting. The overall process would then be limited by another step of the chemical system (enolization, dehydration...) and the rate constant would not follow eq 13. Alternatively, the parameter k_o in eq 12 might be much smaller for 2,4-pentanedione than for other carbonyl compounds. In any case, the slow reaction rate measured for 2,4-pentanedione in this work does not result from measurement or analysis artifacts: If this reaction was fast, it should have resulted in some significant uptake at low or intermediate acid concentration, which was not observed.

The rate constants measured in this work for the aldol condensation of carbonyl compounds in sulfuric acid solutions are thus generally slow. These rate constants can be used to estimate the increase of aerosol mass resulting from the aldol condensation of acetone in typical smog chamber experiments. We will assume in these calculations that the concentration of acetone in the gas is $C_o = 2$ ppmV (1 ppmV = 10^{-6} V/V), the volume fraction of the acid aerosol 5×10^{-11} (cm^3/cm^3), its composition 50 wt % H_2SO_4,[3] and the temperature 298 K. At this temperature, the Henry's law coefficient of acetone in the aerosol is about 65 $Matm^{-1}$.[21] The results of this work indicate that, under these conditions, $k_{liq}^{II} \sim 3.3 \times 10^{-4}$ M^{-1} s^{-1} and thus $k_{liq} \sim 5 \times 10^{-9}$ s^{-1}. Assuming that eq 5 is valid for the

aerosol, which is probably the case for slow reactions and particles saturated in reactants,[25] we can estimate that $k_{l_{gas}} \sim 4 \times 10^{-16}$ s^{-1}. For an aerosol of specific surface of 10^{-7} cm^{-1}, this corresponds to an uptake coefficient of $\gamma \sim 6 \times 10^{-13}$. The flux of molecules leaving the gas phase to increase the aerosol mass is $k_{l_{gas}} \times C_o \sim 2.4 \times 10^{-3}$ molecules cm^{-3} s^{-1}. For acetone of molecular weight 59 g mol^{-1}, this flux leads to an increase of mass of 10^{-21} g cm^{-3} after 1 h of experiment. As compared to the 5×10^{-11} g cm^{-3} typical of aerosols in smog chamber experiments,[3] this is a negligible increase of mass. Obviously, this figure would be even smaller under atmospheric conditions, where the concentrations of carbonyl compounds would be even smaller, the temperature lower, and the specific surface and volume of the aerosol smaller as well. The reactions studied in this work seem thus not to be fast enough to account for the enhanced organic aerosol mass observed in smog chambers. The rate constants for other carbonyl compounds, such as the large aldehydes used in ref 3−5, remain, however, to be measured. Reversing the calculation performed above for the same conditions, one can estimate the uptake coefficient necessary to account for the observed increase of aerosol mass: An increase of mass of a factor 2 (that is, 5×10^{-11} g cm^{-3}) after 1 h of experiment would correspond to a flux from the gas phase of 10^8 molecules cm^{-3} s^{-1}. For the same concentrations of acetone, this would be a first-order loss from the gas phase of $k_{l_{gas}} = 2.5 \times 10^{-5}$ s^{-1} and, for a specific aerosol surface of 10^{-7} cm^{-1}, an uptake coefficient of the order of $\gamma \sim 10^{-2}$. Finally, one can note that the increase of the Henry's law coefficient at high acidity mentioned previously might favor the reversible partitioning of the carbonyl species into the aerosol. This effect is, however, significant in fairly concentrated acid only (at least 50 wt % H_2SO_4) and thus unlikely to be important under atmospheric conditions.

V. Conclusion

Measurements of the uptake of acetone, 2-butanone, 2,4-pentanedione, and acetaldehyde in sulfuric acid solutions have identified the occurrence of irreversible reactions in concentrated acid solutions, which were found to follow a second-order kinetics. The rate constants measured in this work and their variations with acidity were generally in very good agreement with the rate constants measured and predicted for the acid-catalyzed aldol condensation of carbonyl compounds, except for 2,4-pentanedione, and provided a good validation of our measurements and analysis. Equation 13 can thus be used to estimate the rate constant of aldol condensation of any carbonyl compound in any acid concentration, to the exception, perhaps, of compounds with exceptionally large enolization constants for which the actual reaction would be slower than predicted. The results of this work suggest that aldol condensation, although a good example of polymer-forming reaction, is not fast enough to account for the organic aerosol yields measured in smog chamber studies. The rate constants for large aldehydes remain, however, to be measured. The large Henry's law coefficients of carbonyl compounds in concentrated acid might favor their partitioning in the condensed phase, but only with fairly acidic particles.

Acknowledgment. We acknowledge Dr. Dan Riemer, University of Miami/RSMAS, for his help with the standards and bubble column measurements and Dr. E. Atlas, University of Miami/RSMAS, for comments on the manuscript. B.N. thanks Dr. Dave Hanson, National Center for Atmospheric Research, for teaching principles of the RWW reactor technique.

Appendix I

This appendix discusses the radial concentration profiles of organic compounds in the acid solutions, X(r,t). We first discuss the profiles in the case of a first-order reaction (rate constant k^I_{liq}). These profiles are solutions of the Fick diffusion equation:

$$\frac{\partial X(r,t)}{\partial t} = D_{liq}\frac{\partial^2 X(r,t)}{\partial r^2} - k^I_{liq}X(r,t) \qquad (14)$$

where D_{liq} is the diffusion coefficient. The complete, time-dependent solution of eq 14 is a combination of "erf" functions, which reaches a steady state when

$$r \ll 2\sqrt{k^I_{liq}D_{liq}}t$$

With $k_{l_{liq}} \sim 10^{-3}$ s^{-1} and $D_{liq} \sim 5 \times 10^{-7}$ cm^2 s^{-1}, this steady state is reached at 90% at the bottom of the solution ($r = 0.01$ cm) for $t \sim 37$ min, which is of the time scale of our measurements. In our experiments, stirring helped reach this steady state even faster. For a liquid of finite thickness at Henry's Law equilibrium with the gas phase at the surface ($X_o = RTHC_o$), the steady state concentration profile is

$$X(r) = X_o\frac{\exp\left[\sqrt{\frac{k^I_{liq}}{D_{liq}}}(0.01 - r)\right] + \exp^{-}\left[\sqrt{\frac{k^I_{liq}}{D_{liq}}}(0.01 - r)\right]}{\exp^{-}\left[\sqrt{\frac{k^I_{liq}}{D_{liq}}}0.01\right] + \exp\left[\sqrt{\frac{k^I_{liq}}{D_{liq}}}0.01\right]} \qquad (15)$$

The parameters given in Table 1 allow one to estimate the quantity $\sqrt{(k^I_{liq}/D_{liq})}$. For example, for acetone in 89.4 wt % H_2SO_4 solution, $\sqrt{(k_{l_{liq}}/D_{liq})} = 94.9$, and the radial concentration gradient is thus $X(0.01)/X_o \sim 67\%$. Generally, the radial concentration gradients predicted by eq 15 were small or negligible in most of our experiments.

For second-order reactions, finding an analytical expression for the radial concentration profile is more complicated. In Appendix III, we show that the quantities $k_{l_{liq}}$ and $k^{II}_{liq}X$ are equivalent at the surface of the liquid and at roughly mid-axial distance of the reactor. This means that in the second part of the reactor, concentrations in the liquid are low enough that a second-order reaction would have less effect on the concentration gradient than what was estimated above for a first-order reaction. In the first part of the reactor, to the contrary, a second-order reaction would be faster than a first-order one, this effect being maximum at the surface of the liquid if radial concentration gradients are indeed present. The correction factor determined in Appendix III means that multiplying $k_{l_{liq}}$ by a factor 3 should provide an upper limit for the rate of the second-order reaction (which, strictly, would apply only at the beginning of the reactor, $z = 0$, and at the surface of the liquid). Multiplying $k_{l_{liq}}$ by 3 in the previous example leads to a slightly larger gradient: $X(0.01)/X_o \sim 40\%$. However, this estimate is really a worst case scenario.

Finally, in addition to the effect to liquid diffusion, the solutions were stirred at a rate of 15 rpm over 30 min, which corresponds to a total of 450 rotations. It is therefore reasonable to assume that, even if diffusion was not sufficient, stirring helped to achieve uniform radial concentration profiles in our experiments.

Appendix II

The object of this appendix is to demonstrate eq 5, which applies only to first-order liquid phase reactions. This demon-

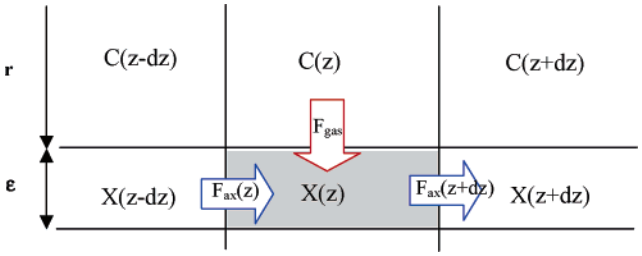

Figure 7. Schematic illustrating the budget made in Appendix II.

stration is based on a budget over fluxes of molecules in the reactor, starting with a small section of reactor of length dz situated in z (Figure 7). To simplify the notation, the thickness of the liquid film will be referred to as ϵ in this appendix, r being the radius occupied by the gas only. The volume of liquid contained in the small section of reactor is $v_{liq} = \pi[(r+\epsilon)^2 - r^2]$, the volume of gas $v_{gas} = \pi r^2\,dz$, and the surface area of the gas−liquid interface $s_{liq} = 2\pi r\,dz$. Three types of fluxes have to be taken into account: (i) the flux of molecules from the gas into the liquid, F_{gas}; (ii) the fluxes due to axial diffusion in the liquid, $F_{ax}(z)$ and $F_{ax}(z+dz)$; and (iii) the flux of molecules consumed by reaction in the liquid, F_{rxn} (Figure 7).

(i) F_{gas} can be determined from the number of molecules crossing the interface s_{liq} during the gas−liquid contact time dt:

$$F_{gas} = -\frac{1}{s_{liq}}\frac{dN}{dt} = -\frac{v_{gas}}{s_{liq}}\frac{dC}{dt} \tag{16}$$

Note that F_{gas} is positive for molecules entering the liquid and therefore of opposite sign of dN/dt. In eq 16, the relationship between contact time and axial distance in the reactor can be expressed explicitly:

$$\frac{dC}{dt} = \frac{\partial C}{\partial z} \times \frac{\partial z}{\partial t} \tag{17}$$

and, using the plug flow approximation

$$\frac{\partial z}{\partial t} = \frac{F}{2\pi r} \tag{18}$$

where F is the volumetric flow ($\sim$50 cm^3 s^{-1}). Thus, the expression of F_{gas} as a function of the gas phase axial concentration gradient, dC/dz, is

$$F_{gas} = -\frac{\partial C}{\partial z}\frac{F}{2\pi r} \tag{19}$$

The gas phase concentration gradient is observed experimentally to be exponential (Figure 3):

$$C(z) = C_o e^{-\nu_{gas} z} \tag{20}$$

with $\nu_{gas} \sim 0.15$ cm^{-1}. The plug flow approximation allows one to express ν_{gas} as a function of k^I_{gas}, the quantity measured experimentally

$$\nu_{gas} = k^I_{gas}\frac{\pi r^2}{F} \tag{21}$$

Equation 20 allows one to calculate the axial gradient:

$$\frac{\partial C}{\partial z} = -\nu_{gas} C = -k^I_{gas}\frac{\pi r^2}{F} C \tag{22}$$

and thus F_{gas}:

$$F_{gas} = k^I_{gas}\frac{\pi r^2}{F} C \times \frac{F}{2\pi r} = k^I_{gas} C \times \frac{r}{2} \tag{23}$$

Note that F_{gas} depends on the gas phase concentration and therefore on z. This flux is much larger at the beginning of the reactor than at the end.

(ii) The fluxes due to axial diffusion in the liquid can be determined from the Fick equation:

$$F_{ax}(z) = -D_{liq}\frac{\partial X}{\partial z} \tag{24}$$

The results of Appendix I (uniformity of radial concentrations in solution and Henry's equilibrium) imply that the axial concentration profiles in the liquid are similar to the ones in the gas, that is, exponential:

$$X(z) = X_o e^{-\nu_{gas} z} \tag{25}$$

$$\frac{\partial X}{\partial z} = -\nu_{gas} X = -k^I_{gas}\frac{\pi r^2}{F} X \tag{26}$$

thus

$$F_{ax}(z) = D_{liq} k^I_{gas}\frac{\pi r^2}{F} X \tag{27}$$

Replacing X by $RTHC$ and assuming $H = 1000$ M atm^{-1} shows that F_{ax} is orders of magnitudes smaller than F_{gas} ($\sim 10^{-4}$ as compared to 1/2) because D_{liq} is very small ($\sim 10^{-7}$ cm^2 s^{-1}). Moreover, the net axial flux of molecules over the small section of liquid is the difference $F_{ax}(z) - F_{ax}(z+dz)$, which is even smaller. The net flux due to axial diffusion is thus negligible as compared to the flux from the gas phase.

(iii) The number of molecules consumed by a first-order reaction in the liquid is

$$\frac{dN}{dt} = v_{liq}\frac{dX}{dt} = v_{liq} k^I_{liq} X \tag{28}$$

Dividing this quantity by the surface area of the liquid gives the corresponding flux:

$$F_{rxn} = \frac{1}{2\pi r\,dz}\frac{dN}{dt} = k^I_{liq} X \frac{\pi[(r+\epsilon)^2 - r^2]\,dz}{2\pi r\,dz} \tag{29}$$

(iv) The axial diffusion fluxes being negligible, the budget on the small section of reactor is simply the equality between F_{gas} and F_{rxn}, which rearranges into

$$k^I_{gas}\pi r^2\,dz = k^I_{liq} RTH\pi[(r+\epsilon)^2 - r^2]\,dz \tag{30}$$

The budget for the whole reactor is obtained by integrating both sides of eq 30 over z. Because none of the parameters on

either side depends on z this integration gives simply

$$k^{I}_{gas}\pi r^2 L = k^{I}_{liq} RTH\pi[(r+\epsilon)^2 - r^2]L \qquad (31)$$

which is eq 5, since $V_{gas} = \pi r^2 L$ and $V_{liq} = \pi[(r+\epsilon)^2 - r^2]L$.

Appendix III

The object of this appendix is, in the case of second-order reactions, to establish the relationship between their rate constant, k^{II}_{liq}, and the first-order rates, k_{liq}, given by eq 5. The equivalent of eq 28 and F_{rxn} in the case of a second-order reaction is

$$\frac{dN}{dt} = \upsilon_{liq}\frac{dX}{dt} = \upsilon_{liq} k^{II}_{liq} X^2 \qquad (32)$$

and

$$F_{rxn} = k^{II}_{liq} X^2 \frac{\pi[(r+\epsilon)^2 - r^2]\, dz}{2\pi r\, dz} \qquad (33)$$

For the small section of reactor, the budget between F_{gas} and F_{rxn} equivalent to eq 30 is then

$$k^{I}_{gas}\pi r^2\, dz = k^{II}_{liq}(RTH)^2 \frac{V_{liq}}{L} C(z)\, dz \qquad (34)$$

The budget for the entire reactor is obtained by integrating both sides of eq 34 over z, using expression 20 for $C(z)$. This leads to

$$k^{I}_{gas} V_{gas} = k^{II}_{liq}(RTH)^2 \frac{V_{liq}}{L} C_o\left[\frac{1 - e^{-\nu_{gas}L}}{\nu_{gas}}\right] \qquad (35)$$

Replacing the expression of k_{liq} given by eq 5 in eq 35 leads to

$$k^{II}_{liq} = \frac{k^{I}_{liq}}{RTHC_o}\left[\frac{L\nu_{gas}}{1 - e^{-\nu_{gas}L}}\right] \qquad (36)$$

k^{II}_{liq} is thus obtained by dividing k_{liq} by the concentration of organic compound in the liquid at an intermediate position in the reactor, determined by the correction factor between brackets. For $L = 18$ cm and $\nu_{gas} \sim 0.15$ cm^{-1}, this factor is about 2.9, which corresponds to the concentration at $z \sim 7$ cm. For the experiments where the uptake was smaller, this correction factor was close to 1.

References and Notes

(1) Pankow, J. F. *Atmos. Environ*. **1994**, *28*, 189.
(2) Griffin, R. J.; Dabdub, D.; Kleeman, M. J.; Fraser, M P.; Cass, G. R.; Seinfeld, J. H. *J. Geophys. Res.* **2002**, *107*, 4334.
(3) Jang, M.; Kamens, R. M. *Environ. Sci. Technol*. **2001**, *35*, 4758.
(4) Jang, M.; Czoschke, N. M.; Lee, S.; Kamens, R. M. *Science* **2002**, *298*, 814.
(5) Jang, M.; Lee, S.; Kamens, R. M. *Atmos. Environ*. **2003**, *37*, 2125.
(6) Limbeck, A.; Kulmala, M.; Puxbaum, H. *Geophys. Res. Lett*. **2003**, *30*, doi: 10.1029/2003GL017738.
(7) Iinuma, B. O.; Gnauk, T.; Hermann, H. *Atmos. Environ*. **2004**, *38*, 761.
(8) Smith, M. B.; March, J. *Advanced Organic Chemistry*; J. Wiley and Sons: New York, 2001.
(9) Liler, M. *Reaction Mechanisms in Sulfuric Acid and Other Strong Acid Solutions*; Academic Press: New York, 1971.
(10) Duncan, J. L.; Schindler, L. R.; Roberts, J. T. *Geophys. Res. Lett.* **1998**, *25*, 631.
(11) Duncan, J. L.; Schindler, L. R.; Roberts, J. T. *J. Phys. Chem. B* **1999**, *103*, 7247.
(12) Kane, S. M.; Timonen, R. S.; Leu, M.-T. *J. Phys. Chem*. **1999**, *103*, 9259.
(13) Klassen, J. K.; Lynton, J.; Golden, D. M.; Williams, L. *J. Geophys. Res*. **1999**, *104*, 26355.
(14) Imamura, T.; Akiyoshi, H. *Geophys. Res. Lett*. **2000**, *27*, 1419.
(15) Michelsen, R. R.; Ashbourn, S. F. M.; Iraci, L. T. *J. Geophys. Res.* **2004**, *109*, doi: 10.1029/2004JD005041.
(16) Baigrie, L. M.; Cox, R. A.; Slebocka-Tilk, H.; Tencer, M.; Tidwell, T. T. *J. Am. Chem. Soc*. **1985**, *107*, 3640.
(17) Lovejoy, E. R.; Huey, L. G.; Hanson, D. R. *J. Geophys. Res*. **1995**, *100*, 18775.
(18) Hanson, D. R.; Lovejoy, E. R. *J. Phys. Chem*. **1996**, *100*, 6397.
(19) Gmitro, J. I.; Vermeulen, T. *Am. Inst. Chem. Eng. J*. **1964**, *10*, 740.
(20) Murphy, D. M.; Fahey, D. W. *Anal. Chem.* **1987**, *59*, 2753.
(21) Noziere, B.; Riemer, D. *Atmos. Environ*. **2003**, *37*, 841.
(22) Apel, E. C.; Calvert, J. G.; Greenberg, J. P.; Riemer, D.; Zika, R.; Kleindienst, T. E.; Lonneman, W. A.; Fung, K.; Fujita, E. *J. Geophys. Res.* **1998**, *103*, 22281.
(23) Cox, R. A.; Yates, K. *J. Am. Chem. Soc*. **1978**, *100*, 3861.
(24) Carslaw, K. S.; Clegg, S. L.; Brimblecombe, P. *J. Phys. Chem*. **1995**, *99*, 11557. Model web site: http://www.hpc1.uea.ac.uk/~e770/aim.html.
(25) Hanson, D. R.; Ravishankara, A. R.; Solomon, S. *J. Geophys. Res*. **1994**, *99*, 3615.
(26) (a) Williams, L. R.; Long, F. S. *J. Phys. Chem*. **1995**, *99*, 3748. (b) Klassen, J. K.; Hu, Z.; Williams, L. R. *J. Geophys. Res.* **1998**, *103*, 16197. (c) Kane, S. M.; Leu, M.-T. *J. Phys. Chem. A* **2001**, *105*, 1411.
(27) Chiang, Y.; Hojatti, M.; Keeffe, J. R.; Kresge, A. J.; Schepp, N. P.; Wirtz, J. *J. Am. Chem. Soc*. **1987**, *109*, 4000.
(28) (a) Guthrie, J. P. *Can. J. Chem*. **1979**, *57*, 1177. (b) Dubois, J.-E.; El-Alaoui, M.; Toullec, J. *J. Am. Chem. Soc*. **1981**, *103*, 5393. (c) Chiang, Y.; Kresge, A. J.; Schepp, N. P. *J. Am. Chem. Soc*. **1989**, *111*, 3977.
(29) Keeffe, J. R.; Kresge, A. J.; Schepp, N. P. *J. Am. Chem. Soc*. **1990**, *112*, 4862.
(30) Moriyasu, M.; Kato A.; Hashimoto, Y. *J. Chem. Soc., Perkin Trans. 2* **1986**, 515.
(31) Cox, R. A.; Smith, C. R.; Yates, K. *Can. J. Chem*. **1979**, *57*, 2952.
(32) Eistert, B.; Merkel, E.; Reiss, W. *Chem. Ber*. **1954**, *87*, 1513.